

Apr. 27, 2001

Hua Zhong

CEM 924

Final Report

16. How does photoemission from adsorbed Xe (PAX) work and what can it tell us?

Photoemission of Adsorbed Xenon (PAX)

— *A probe for detecting the local work function*

1. Introduction

The characterization of heterogeneous surfaces on the atomic scale is an important requirement to understand the physics and chemistry of real surfaces. Photoemission of adsorbed xenon, i.e. PAX, is a reversible, non-destructive technique, which can identify and titrate different adsorption sites. Compared with scanning tunneling microscopy (STM), PAX can provide information not only about the relative abundance of specific surface sites, but also about their local work function.^[1]

PAX can be applied to the surfaces of metal ^{[2][3]}, semiconductor ^{[4][5]} or mineral such as FeS₂^{[6][7]}. It can be used to detect the structural or chemical defects ^{[2][3][6][7]}, the active sites of catalysts^[8], the metal film growth^[5], and so on.

2. Principles of PAX

At temperatures below 80K, xenon atoms can physisorb on any solid surface.^[1] At the low background pressure, xenon atoms preferentially adsorb on the surface site of high adsorption energy. With the increasing background pressure, xenon atoms successively populate on other kinds of surface sites according to the adsorption energies until they form a monolayer on the surface. At higher background pressure, xenon atoms can form a bilayer on the surface. Fig.1 shows two xenon atoms adsorbed on two kinds of surface sites, i.e. step and terrace. Both of the two xenon atoms excite valance or core photoelectrons with the incident UV radiation or x-ray, respectively. Since they adsorb on sites of different local work function, the binding energy with respect to Fermi level E_B^v varies. Therefore, the x-ray photoemission spectroscopy (XPS) or the ultraviolet photoemission spectroscopy (UPS) of the adsorbed xenon can provide information of the underlying surface.

The *5p* valence band UPS spectrum of a complete monolayer of Xe on a well defined Pd(110) surface is shown in Fig.2^[1]. Spectrum a) first shows the UPS spectrum of the valence band region of the bare palladium substrate with dominant emission from the *4d* band close to the Fermi level. Spectrum b) shows the UPS spectrum of the same Pd(110) surface covered with one complete monolayer of xenon. The two sharp and intense extra peaks (shaded) between 5eV and 8eV arise from the adsorbed xenon atoms. Spectrum c) is obtained by subtracting spectrum a)

from spectrum b), which is the photoemission spectrum of the Xe adsorbed on Pd(110).

Since the photoemission spectrum measures the binding energy with respect to the Fermi level E_B^F , the binding energy with respect to the vacuum level E_B^V can be obtained by adding E_B^F with the macroscopic work function of the surface ϕ . Table 1 lists the macroscopic work functions ϕ , and electron binding energies with respect to the Fermi level E_B^F of the $5p_{1/2}$ level of Xe adsorbed on the various homogeneous surfaces. Note the approximate invariance of the E_B^V compared to ϕ and E_B^F , which is because of the weak Xe/substrate interaction and the big Xe diameter.

Table 1 The approximate invariance of the E_B^V of $5p_{1/2}$ level of Xe adsorbed on various surfaces^[1]

Surface	ϕ /eV ⁽¹⁾	E_B^F /eV	$E_B^V = \phi + E_B^F$
Pd(110)	5.20	7.03	12.23
Pd(100)	5.65	6.75	12.40
Pd(111)	5.95	6.47	12.42
Pt(111)	6.40	5.90	12.30
Ir(100)(1×1)	6.15	6.24	12.39
Ir(100)(5×1)	6.00	6.38	12.38
Re(0001)	6.65	5.40	12.15
Ru(0001)	5.52	6.76	12.28
W(001)	4.50	7.90	12.40
W(110)	5.10	7.15	12.25
Ni(110)	4.65	7.75	12.40
Ni(100)	5.30	6.90	12.20
Ni(111)	5.40	6.80	12.20
Cu(110)	4.48	7.80	12.28
Cu(111)	4.90	7.10	12.00 ⁽²⁾
		7.30	12.20
Ag(111)	4.72	7.27	11.99 ⁽²⁾
		7.62	12.34
Ag(100)	4.65	7.68	12.33
Au(111)	5.68	6.72	12.40
Al(111)	4.48	7.74	12.22
Al(110)	4.45	7.80	12.25
K(poly)	2.20	10.21	12.41
Cs(poly)	1.80	10.50	12.30
ZnO(000-1)O	4.35	8.00	12.35
ZnO(0001)Zn	3.75	8.70	12.45
ZnO(10-10)	4.05	8.25	12.30
n-Si(111)	4.65	7.70	12.35
p-Si(111)	5.55	6.80	12.35

n-Si(100)	4.60	7.70	12.30
Adsorbed Xe			12.30 ± 0.15
Xe gas			13.40
$-E_R = E_B^N (\text{adsorbed Xe}) - E_B^N (\text{Xe gas}) = 1.1 \text{ eV}^{(3)}$			

- (1) The ϕ values are determined according to Equation $\phi = \chi - E_{B^{wgx}}^k$.
- (2) On Cu(111) and Ag(111), adsorbed Xe was found to undergo a 2d gas → 2d solid phase transition, which affects E_B^k . The lower E_B^N values correspond to the 2d gas phase; the higher E_B^N values to the 2d solid phase on these two surfaces.
- (3) $-E_R$ denotes the extra atomic relaxation at the surface. The absolute difference of 1.1 eV between the E_B^N ($5p_{1/2}$) values in the adsorbed versus the gas phase is due to a combination of a minor initial state bonding shift and a dominant final state relaxation shift. [9]

Table 2 lists the macroscopic work functions ϕ , and electron binding energies with respect to the Fermi level E_B^k of the $4d_{5/2}$ level of Xe adsorbed on the various homogeneous metal surfaces. Note the approximate invariance of the E_B^N compared to ϕ and E_B^k .

Table 2 The approximate invariance of the E_B^N of $4d_{5/2}$ level of Xe adsorbed on various surfaces [1]

Surface	ϕ /eV ⁽¹⁾	E_B^k /eV	$E_B^N = \phi + E_B^k$
Pd(111)	5.95	60.22	66.17
Pd(100)	5.65	60.50	66.15
Gd(0001)	3.30	62.80	66.10
Ru(001)	5.44	60.74	66.18
1 ML Cu/Ru(001)	4.86	61.33	66.19
Adsorbed Xe			66.15 ± 0.05

- (1) The ϕ values are determined according to Equation $\phi = \chi - E_{B^{wgx}}^k$.

It is the observation of the substrate independence of the Xe electron E_B^N that provides the basis of PAX as a technique for characterizing heterogeneous surfaces. [9] Fig.3a) shows the energy diagram for xenon atoms adsorbed on homogeneous surfaces with differing work function. Since E_B^N of adsorbed xenon atoms is constant and substrate independent, the potential well of an adsorbed xenon atom floats up and down as a whole with the vacuum level, which has received strong theoretical support by self-consistent charge density calculations for a single xenon atom on a jellium surface. [10] Since the Fermi levels E_F of both surfaces are aligned through the spectrometer, the following equation is obtained: $E_B^{k,1,2} = -\phi_{1,2}$. [9] Thus, $E_B^{k,1,2}$ reflects the work function difference between two homogeneous surfaces.

Equation $E_B^{k,1,2} = -\phi_{1,2}$ also holds for xenon adsorbed on various kinds of sites on

heterogeneous surfaces. [9] In this case E_B^x is determined by the difference in local work function ϕ_{loc} between two sites A and B with work functions ϕ_{loc^A} , and ϕ_{loc^B} on the heterogeneous surface, which is shown in Fig.3b).

The difference of the local work function results in the coexistence of sets of Xe emission lines, which is the focus of the PAX spectra studies. Fig.4 [9] shows the PAX spectra of Xe adsorbed on the PtPd alloy surface. At low coverages, xenon atoms preferentially adsorb on the palladium sites. When the coverage reaches 2L, the Xe emission lines related with platinum sites emerge, which means xenon atoms start to adsorb on the platinum sites. The distance between two $5p_{1/2}$ peaks, or that between two $5p_{3/2}$ peaks represents E_B^x , which equals the difference of the local work function between platinum sites and palladium sites, i.e. ϕ_{loc} .

3. Instrumentation of PAX

The PAX spectra can be obtained with UPS or XPS instrumentation in an ultrahigh vacuum (UHV) chamber.

The sample is held by tantalum clips to a 3.8cm diameter molybdenum plate mounted on the liquid nitrogen reservoir. The temperature is measured with a chromel-alumel thermocouple pressed to the front of the sample by the tantalum clips. The PAX spectra are taken after the sample is cooled to 79K by the liquid nitrogen reservoir integrated into the sample holder and the Xe is admitted into the chamber. [2] At the temperature of 79K, Xe will not condense, so a background pressure of Xe needs to be maintained in the apparatus to establish a steady-state concentration of adsorbed Xe. [6]

The PAX $5p$ spectra are acquired with UV-radiation from a He-discharge lamp (He I = 21.22eV) and detected with an angle-integrating hemispherical electron energy analyzer.[1]

The PAX $4d/3d$ spectra are acquired with Mg K_α radiation (1253.6eV) from a dual Mg anode and detected with a hemispherical electron energy analyzer. [2] High-resolution PAX $4d/3d$ spectra require the use of synchrotron radiation. [1]

4. Example: bimetallic Cu/Ru powder catalyst [1]

PAX can be applied to real surfaces such as from metal powder catalysts. The information obtained from the PAX spectra about the surface defect density and the local work function at the defect sites can be correlated with adsorption and catalytic activity of catalyst surface.

Fig.5a) shows PAX spectra of the ruthenium powder of ~500 angstroms in diameter, which

was pressed onto a Pt-foil by means of a sapphire pestle. For comparison, Fig.5b) shows PAX spectra of a defective Ru(001) surface which was prepared by bombarding the single crystal surface with 2keV argon ions. The ion dose was equivalent to about one-half of a monolayer. Both sets of spectra are surprisingly similar, in that both show the successive population of surface defects at higher binding energy and of intact Ru(001) patches at lower binding energy. The value $E_B^k(5p_{1/2})=6.8\text{eV}$ from the Ru(001) patches in both cases is identical to the value from a perfect Ru(001) single crystal surface. The value of $E_B^k(5p_{1/2})=7.3\text{eV}$ for the defect sites is identical on both the ruthenium powder particles and the sputter-roughened Ru(001) surface. It suggests a local work function decrease of $\sim 500\text{meV}$ near the defect sites.

The highest spectra of Fig.5a) and 5b) correspond to completion of the monolayer of Xe on the respective sample. The partial intensity arising from the xenon atoms at defect sites is larger on the powder sample than on the sputter-roughened Ru(001) surface. According to a quantitative analysis of the spectra in Fig.5a) about 70% of the total powder surface still consisted of perfect Ru(001) sites.

The $5p$ spectra of Xe adsorbed at different coverages on bimetallic Cu/Ru powder particles are displayed in Fig.5c). This sample was prepared by deposition of approximately 0.5ML of copper on the ruthenium powder. During copper deposition the powder substrate was kept at a temperature of 100K and was subsequently annealed at 650K prior to Xe adsorption. The highest spectrum in Fig.5c) is taken to represent saturation of the Xe monolayer. The spectra show no resolved peak associated with copper island on ruthenium surface. Consequently, the conclusion is drawn that the copper is highly dispersed over the surface of the ruthenium powder.

5. Advantages and disadvantages of PAX

5.1. Advantages

The photoemission derived electron binding energies E_B^k of adsorbed xenon atoms are sensitive to the local work function on heterogeneous surfaces. Experiments with well defined stepped surfaces as well as theoretical estimates based on simple electrostatic grounds have led to a quantified description of the term “local”: Adjacent sites or patches of different work function can be as small as ~ 10 angstroms in diameter to still be distinguished by the photoemission of adsorbed xenon atoms. [9] The lateral resolution of PAX is of the order of the xenon diameter, which means that sites of different work function that are only 5 angstroms apart may be distinguished by PAX. [1]

Under appropriate pressure and temperature conditions xenon tends to form hexagonally close-packed overlayers of known atom density (Xe atoms/cm²). Consequently, at monolayer saturation the relative PAX spectra intensities of different Xe states on a heterogeneous surface may be converted into absolute densities of each kind of site.

Because of the weak interaction between a xenon atom and any substrate and the low temperatures involved, no adsorption induced modifications of the surface such as displacement reactions, surface reconstruction or segregation effects, influence the measurements as do strong adsorbates like O₂, H₂, CO, etc. in chemisorption titration.

Meanwhile, the combination of several other properties makes xenon atoms particularly favorable to be used as the local work function probe rather than any other rare or weakly absorbed gas.

Among the rare gases Xe exhibits the highest induced dipole moment and adsorption energy (up to ~ 10kcal/mol). Xe also has the largest diameter, which results in highest coordination to the surface. This, together with the high mobility of adsorbed xenon atoms, permits highest selectivity in site population according to adsorption energy.

Among the rare gases Xe exhibits the largest spin-orbit separation between the $p_{3/2}$ and $p_{1/2}$ valence states, i.e., 1.3eV. Concentrating on the sharp $5p_{1/2}$ peak, which can perfectly well be fitted by a Lorentzian function, provides the best possible resolution between coexisting Xe adsorption states associated with differing surface sites.^[9]

5.2 Disadvantages

Limitations of the PAX technique are the fact that the substrate should be conducting in order to avoid charging effects during the photoemission experiment, and that the number of differing sites should not exceed two or three in order to arrive at a confident decomposition of the total Xe emission into partial contributions of individual Xe adsorption states.^[9]

And PAX does not provide real space images of surface heterogeneities.^[1]

Reference:

- [1] K. Wandelt, Atomic scale surface characterization with photoemission of adsorbed xenon (PAX), Springer Ser. Surf. Sci., 22 (Chem. Phys. Solid Surf. 8), 289-334, 1990
- [2] G. P. Malafsky, S. S. Fu, D. S. Y. Hsu, Photoemission of adsorbed xenon study of surface defects generated by ion bombardment of Ni(111), J. Vac. Sci. Technol. A 10(6), 3472-3477, 1992
- [3] G. P. Malafsky, The effect of sputter temperature on vacancy island behavior on Ni(111)

- measured by photoemission of adsorbed xenon, *Surface Science*, 306(1-2), L539-L544, 1994
- [4] G. Haugstad, A. Raisanen, X. Yu, L. Vanzetti, A. Franciosi, Photoemission study of adsorbed Xe on GaAs(110), HgTe(110), and $\text{Hg}_{1-x}\text{Cd}_x\text{Te}$ (110) surfaces, *Physical Review B*, 46(7), 4102-4109, 1992
- [5] A. Franciosi, A. Raisanen, G. Haugstad, G. Ceccone, X. Yu, Probing island growth and coalescence at metal-semiconductor interfaces, *Physical Review B*, 41(11), 7914-7917, 1990
- [6] J. M. Guevremont, D. R. Strongin, M. A. A. Schoonen, Photoemission of adsorbed xenon, x-ray photoelectron spectroscopy, and temperature-programmed desorption studies of H_2O on FeS_2 (100), *Langmuir*, 14, 1361-1366, 1998
- [7] J. M. Guevremont, D. R. Strongin, M. A. A. Schoonen, Effects of surface imperfections on the binding of CH_3OH and H_2O on FeS_2 (100): using adsorbed Xe as a probe of mineral surface structure, *Surface Science*, 391, 109-124, 1997
- [8] T. V. W. Janssens, G. R. Castro, K. Wandelt, J. W. Niemantsverdriet, Surface potential around potassium promoter atoms on Rh(111) measured with photoemission of adsorbed Xe, Kr and Ar, *Physical Review B*, 49(20), 14599-14609, 1994
- [9] K. Wandelt, Surface characterization by photoemission of adsorbed xenon (PAX), *J. Vac. Sci. Technol. A* 2(2), 802-807, 1984
- [10] N. D. Lang and A. R. Williams, Theory of local-work-function determination by photoemission from rare-gas adsorbates, *Phys. Rev. B* 25, 2940-2942, 1982

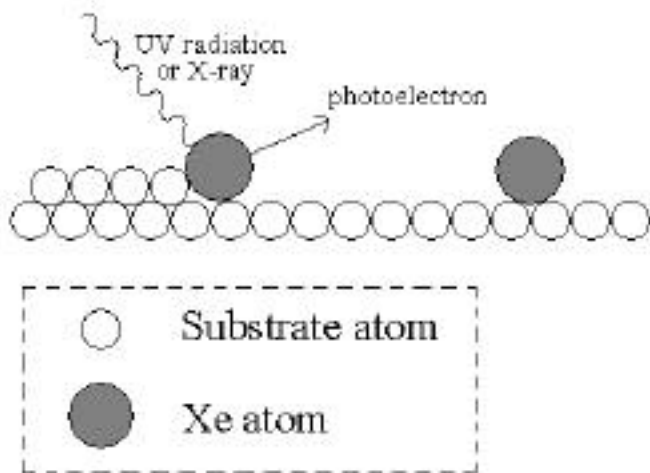


Fig.1 Two xenon atoms adsorbed on surface step site and surface terrace site.

- Fig.2 a) UV photoemission spectra of a clean Pd(110) surface;
 b) UV photoemission spectra of a Pd(110) surface covered with a Xe monolayer;
 c) The Xe induced $5p_{3/2, 1/2}$ emission (shaded) is accentuated by subtract a) from b).

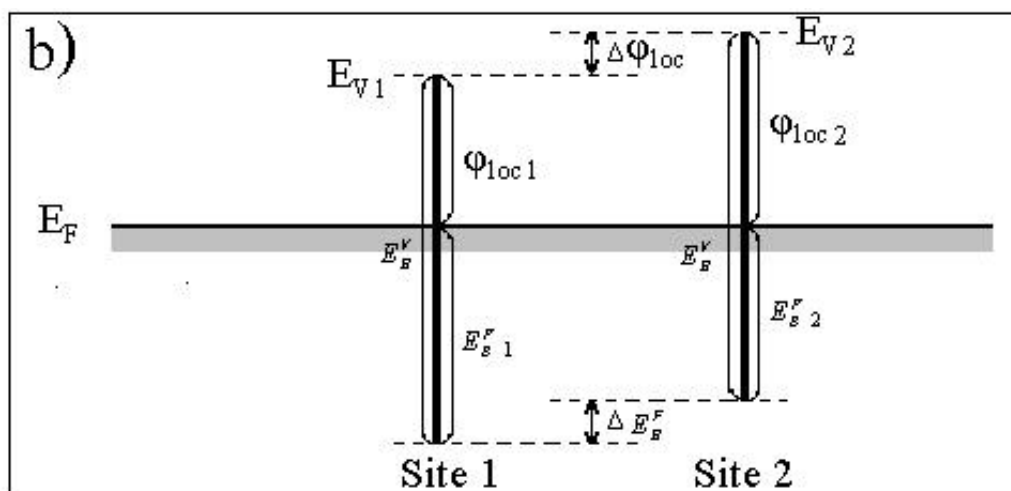
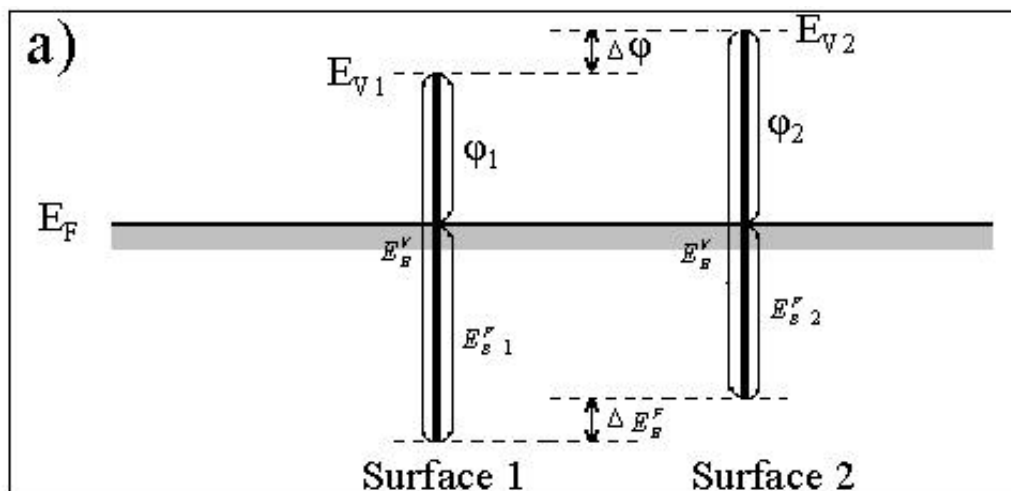


Fig.3 The energy diagram for xenon atoms adsorbed a) on two surfaces with different work function and b) on two sites with different work function of the heterogeneous surface.

Fig.4 Xe ($5p_{3/2, 1/2}$) photoemission spectra from xenon adsorbed on a binary PtPd surface as a function of coverage. At low coverage ($\leq 1\text{L}$) only Pd-like sites are populated, while at higher coverages both Pd- and Pt-like sites are occupied.

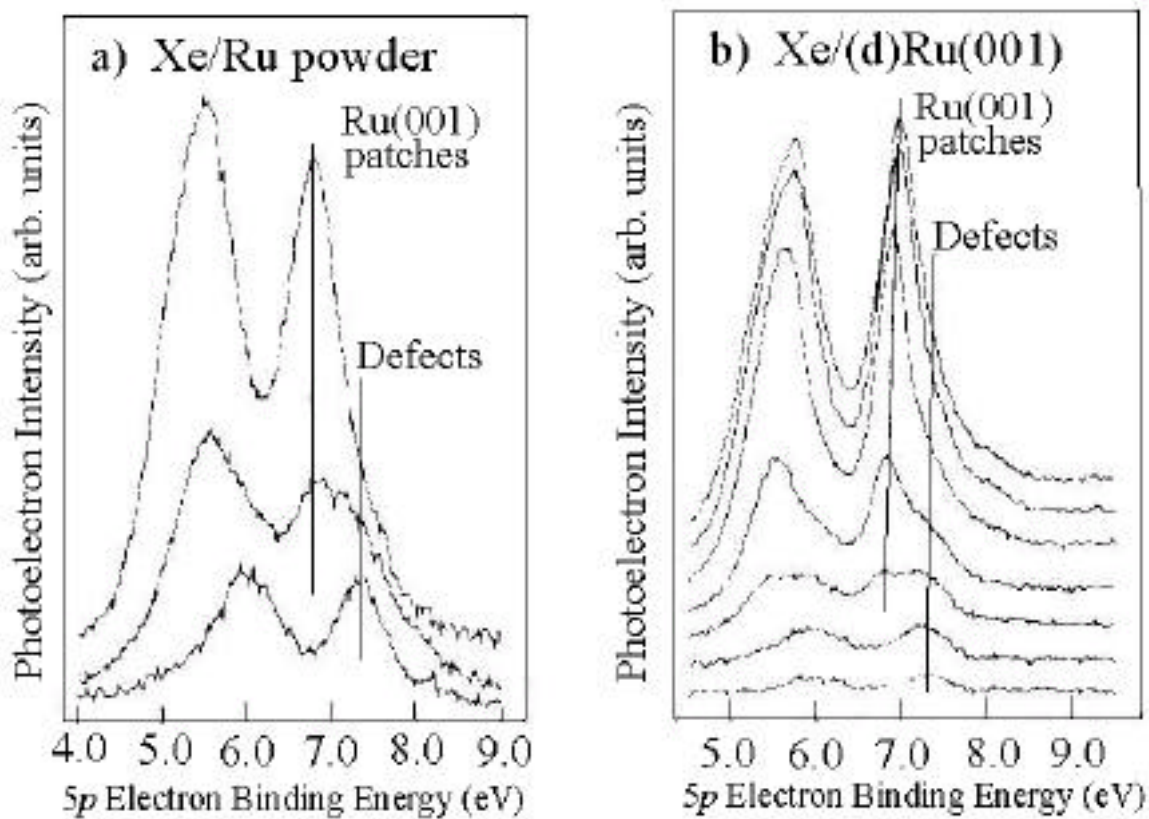


Fig. 5 Xe ($5p_{3/2, 1/2}$) spectra from Xe adsorbed a) on metallic Ru powder particles; b) on a sputter-roughened Ru(001) surface; and c) on bimetallic Cu/Ru powder particles. The highest spectrum corresponds to a complete Xe monolayer in these three cases. Note the sequential population of defect sites and intact Ru(001) patches.